# Coupling the Qbox and WEST codes

H. Ma[1,2], N. L. Nguyen[1], G. Galli[1,2,3], M. Govoni[1,3], F. Gygi[4]

[1]Institute for Molecular Engineering, University of Chicago, Chicago, IL 60637 [2]Department of Chemistry, University of Chicago, Chicago, IL 60637
[3]Materials Science Division, Argonne National Laboratory, Lemont, IL 60439 [4]Department of Computer Science, University of California Davis, Davis, CA 95616.

## Introduction

**Qbox** First-Principles Molecular Dynamics

**Qbox is a massively parallel implementation of first-principles molecular dynamics (FPMD) based on the plane-wave pseudopotential formalism.**

**Code features:**
- **Efficient hybrid DFT calculations using the recursive subspace bisection (RSB) technique**
- **Simulation in arbitrary electric field**
- **Calculation of vibrational spectra (IR, Raman) and ionic conductivity**
- **Calculation of thermal conductivity**

**WEST is a massively parallel code for many body perturbation theory calculations.**

**Code features:**
- **Large-scale *GW* calculation without explicit calculation of empty electronic states**
- **Low-rank decomposition of dielectric matrix**
- **Scalar-relativistic and full-relativistic calculations**
- **GW starting from semi-local and hybrid DFT**
- **GW with full frequency integration**

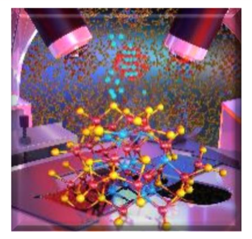

FPMD simulations of all inorganic nanoparticles (InAs in SnS matrix). Scalise et al.. *Nature Nano.* 2018.

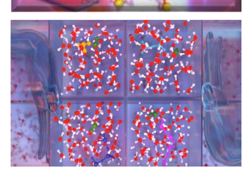

FPMD simulations of vibrational spectra and ionic conductivity of water in extreme conditions. Rozsa et al.. *PNAS.* 2018.

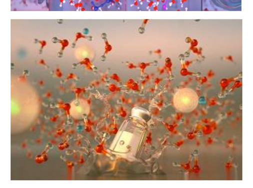

FPMD simulations of water and salt solutions with hybrid functionals. Gaiduk et al. *JPCL.* 2017; *JPCL.* 2018.

FPMD+*GW* calculations of electron affinity of water. Gaiduk et al. *Nature Comm.* 2018.

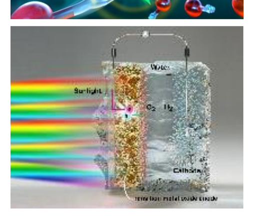

FPMD+*GW* simulations of photoanodes ($WO_3$) for water splitting. Gerosa et al. *Nature Mat.* 2018

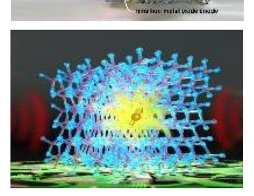

*GW* calculations of defects in semiconductors for qubit design. Seo et al. *Sci. Rep.* 2016; *Nature Comm.* 2016; *PRM.* 2017.

## Qbox-WEST coupling

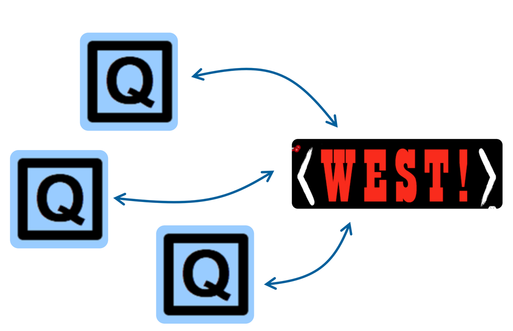

**Coupling the Qbox and WEST codes:**
- **WEST performs iterative diagonalization of response functions within or beyond the random phase approximation.**
- **Qbox in client server mode serves as an efficient DFT engine performing calculations in finite electric fields.**
- **The scheme is readily applicable to hybrid functional calculations.**
- **Orbital localization techniques implemented in Qbox reduce the computational cost.**
- **The coupling can be performed in parallel, with WEST coupled simultaneously with multiple copies of Qbox.**

**The coupling between Qbox and WEST relies on a finite-field approach to evaluate density response functions ($\chi_0$, $\chi_{RPA}$ and $\chi$).**

$$\chi = \chi_0 + \chi_0(v_c + f_{xc})\chi \qquad \chi_{RPA} = \chi_0 + \chi_0 v_c \chi$$

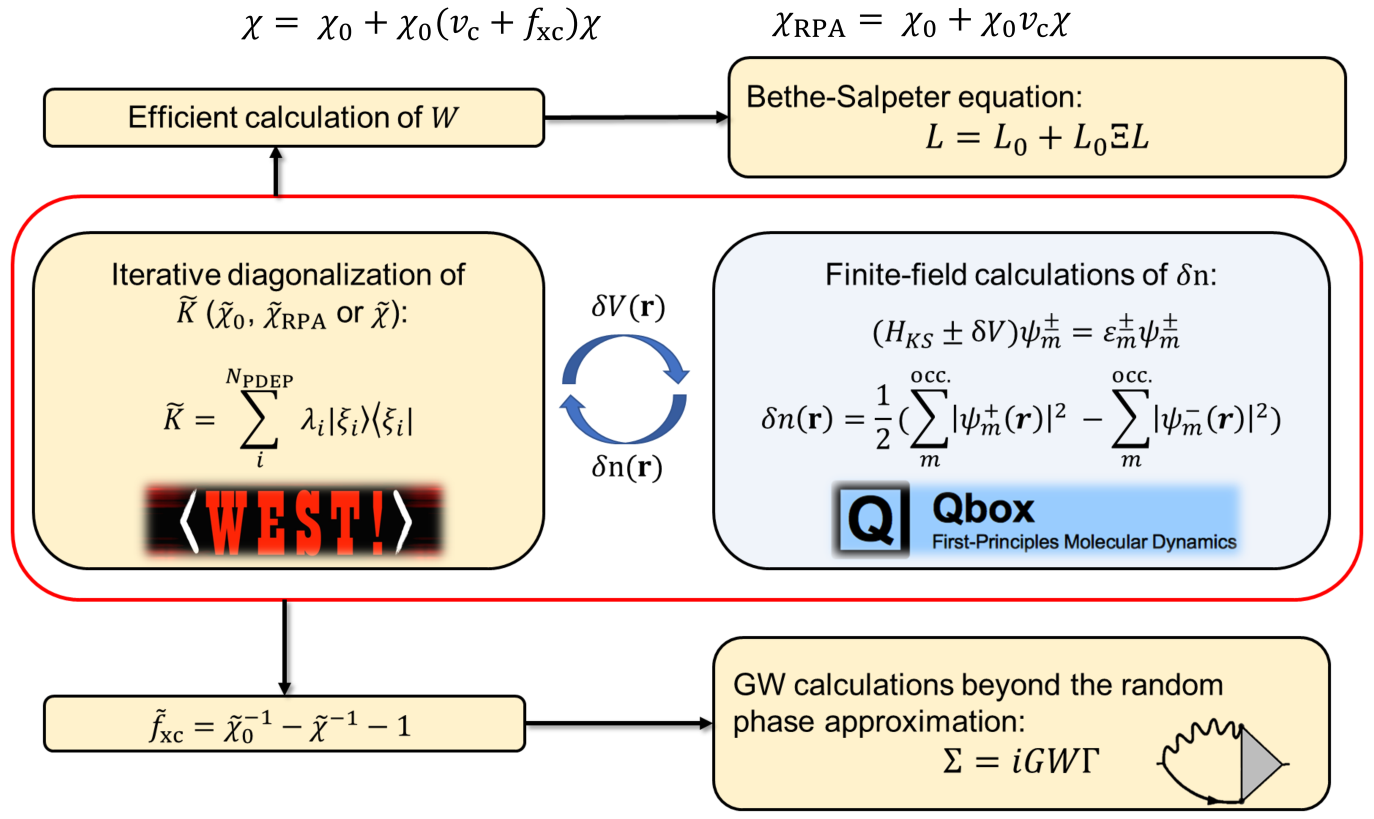


**Code coupling verification:**

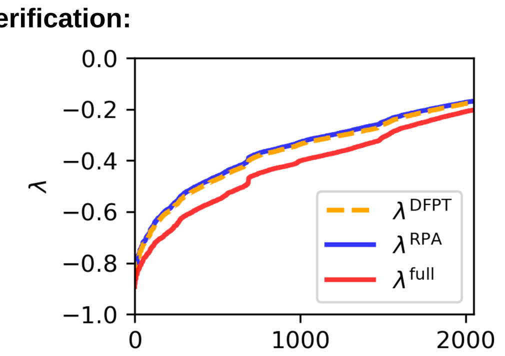


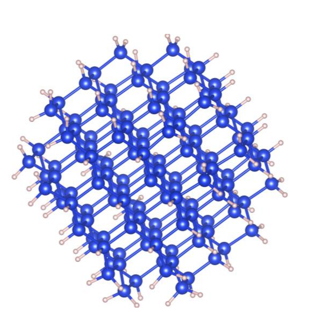

**WEST was coupled to 240 Qbox instances to perform the calculation.**

**First 2048 eigenvalues of the density response function for a $Si_{147}H_{100}$ nanoparticle.**

## *GW* calculations beyond the random phase approximation

**Most *GW* calculations are performed within the random phase approximation (RPA) where the exchange-correlation kernel $f_{xc}$ is neglected in the density response function $\chi$. Based on finite-field calculations performed by coupling Qbox and WEST, $\chi$ can be evaluated beyond the RPA in a straightforward manner.**

**Eigenvalues of $\chi$ for Ar, $SiH_4$ and $CO_2$ molecules computed within and beyond the RPA:**

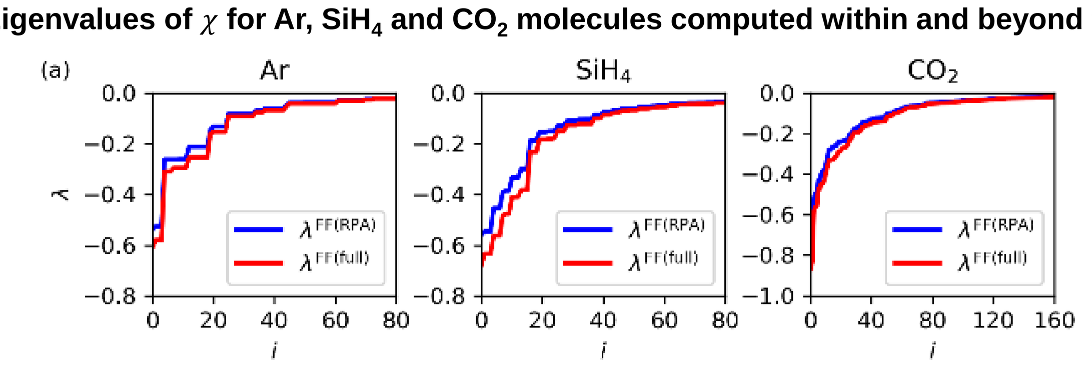


**The kernel $f_{xc}$ can be computed by inverting the Dyson equation connecting $\chi_0$ and $\chi$. Semi-local and hybrid functionals are treated on an equal footing:**

$$f_{xc} = \chi_0^{-1} - \chi^{-1} - v_c$$

**The $f_{xc}$ matrices for Ar, SiH4 and CO2 molecules in the space of $\chi_0$ eigenpotentials:**

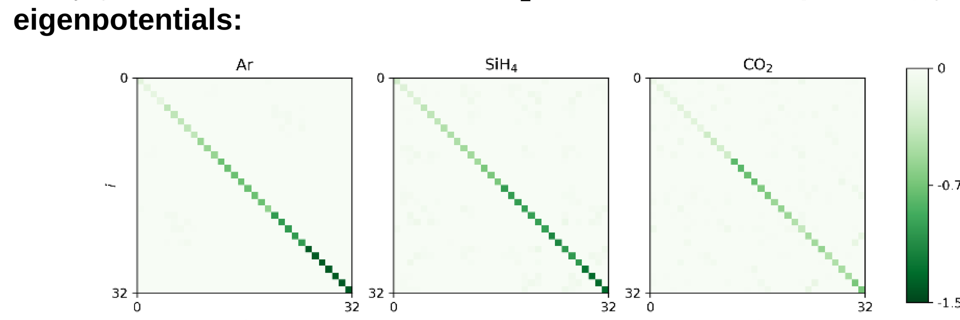


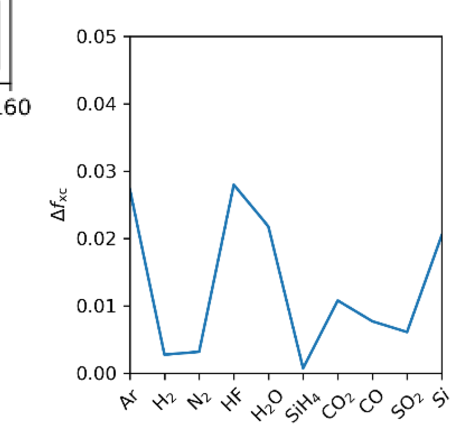

**Comparison between finite-field and analytical evaluation of $f_{xc}$ at the LDA level. Small mean relative difference ($\Delta f_{xc}$) indicates a good accuracy of the finite-field approach adopted to compute $f_{xc}$.**

***GW* calculations beyond the RPA may be performed using $f_{xc}$ computed from coupling the Qbox and WEST codes:**

$$G_0W_0^{RPA} \qquad \chi_{RPA} = \chi_0 + \chi_0 v_c \chi$$

$$G_0W_0^{f_{xc}} \qquad \chi = \chi_0 + \chi_0(v_c + f_{xc})\chi$$

$$G_0W_0\Gamma_0 \qquad \chi_\Gamma = [v_c - v_c\chi_0(v_c + f_{xc})]^{-1} - v_c^{-1}$$

$$\Sigma_{xc}(r, r'; \omega) = \int \frac{d\omega}{2\pi} G(r, r'; \omega + \omega') W(r, r'; \omega')$$

$$G(r, r'; \omega) = \left\langle r \left| \frac{1}{\omega - H} \right| r' \right\rangle$$

$$W(r, r'; \omega) = \int dr'' [\delta(r, r'') + \chi(r, r''; \omega)] v_c(r'', r')$$

**Vertical ionization potential (VIP) and vertical electron affinity (VEA) for molecules: GW100 set**

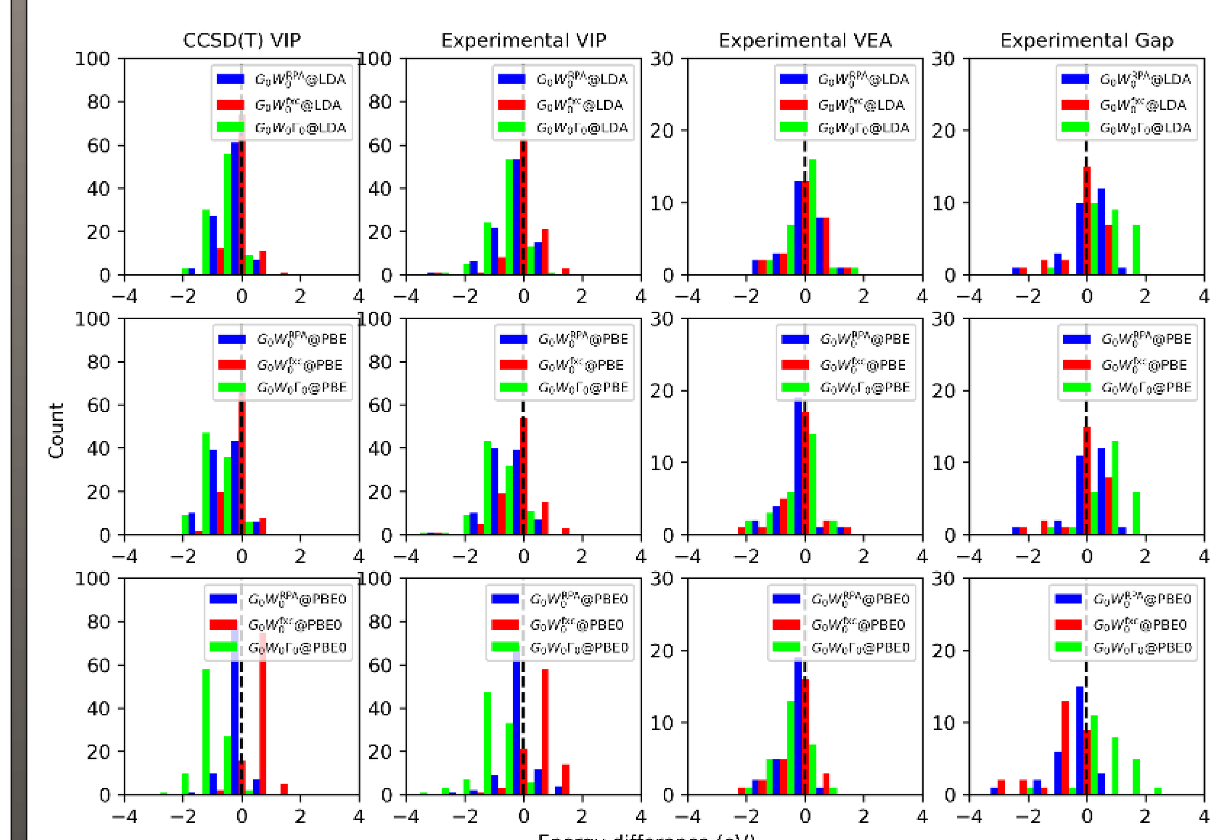


**Quasiparticle corrections for the VBM and CBM of solids**

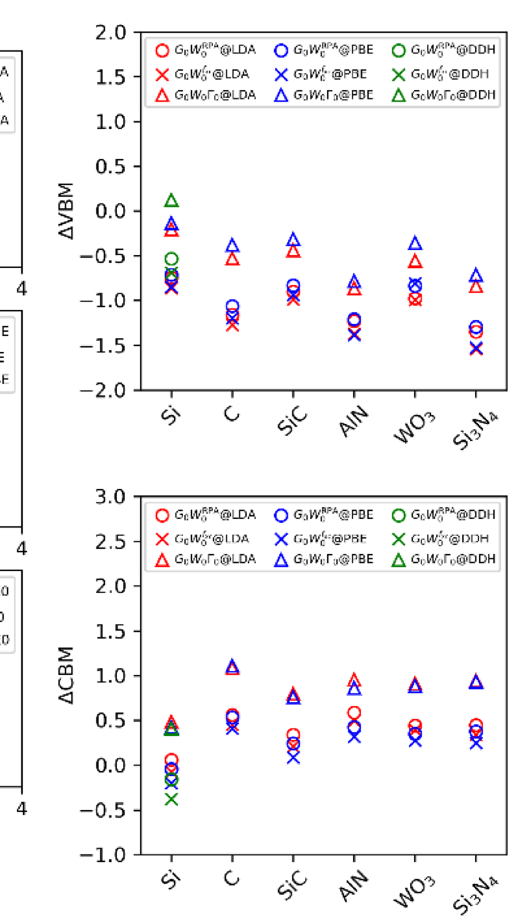


**We developed a scheme to renormalize $f_{xc}$ to accelerate the convergence of $G_0W_0\Gamma_0$ calculations:**

$$\tilde{f}_{xc} = \sum_i^{N_{PDEP}} f_i |\zeta_i\rangle\langle\zeta_i|$$

$$\tilde{f}'_{xc} = \sum_i^{N_{PDEP}} \max(f_i, -1) |\zeta_i\rangle\langle\zeta_i|$$

**The eigenvalues of the renormalized $f_{xc}$ are larger than or equal to the negative of the bare Coulomb interaction, thus guaranteeing the rapid convergence of $G_0W_0\Gamma_0$ quasiparticle energies.**

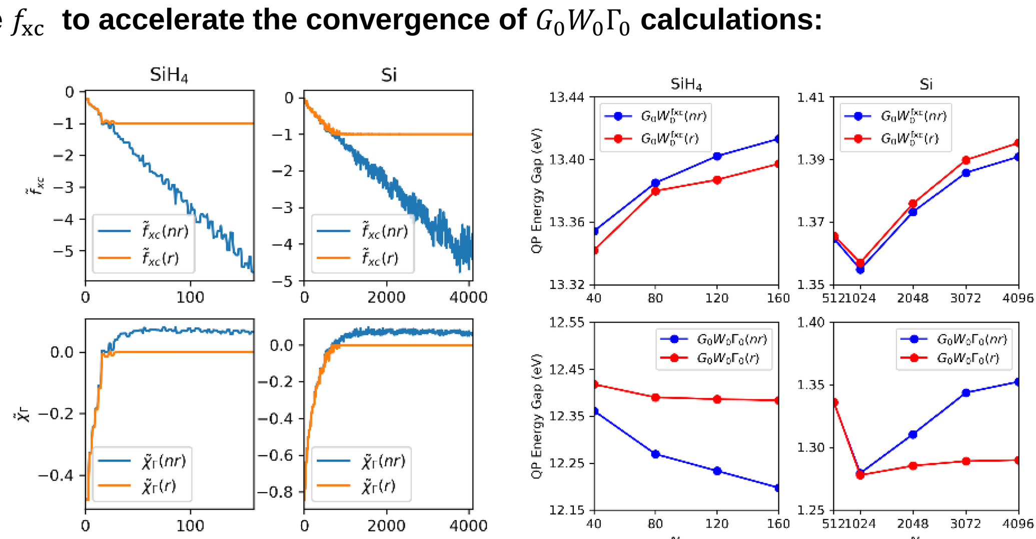


**$f_{xc}$, $\chi_\Gamma$ and quasiparticle energies for the $SiH_4$ molecule and bulk Si.**

## Bethe-Salpeter Equation

**Solution of the Bethe-Salpeter equation (BSE) provides valuable insight into the optical spectra of molecules and solids. We developed an efficient approach to solve the BSE, based on the Liouville-Lanczos algorithm and finite-field calculations. This approach avoids the explicit summation over empty electronic states and altogether the calculation of the dielectric matrix. The screened Coulomb interaction *W* is obtained from finite-field calculations, using the coupling between the Qbox and WEST codes.**

**We verified our BSE approach by computing the singlet excitation energies (Δ) of the 28 molecules of the Thiel's set:**

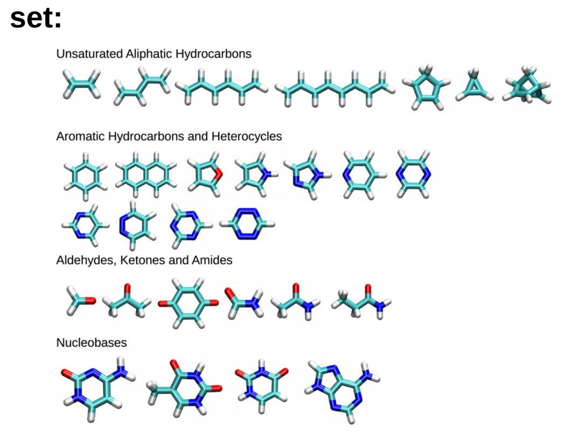


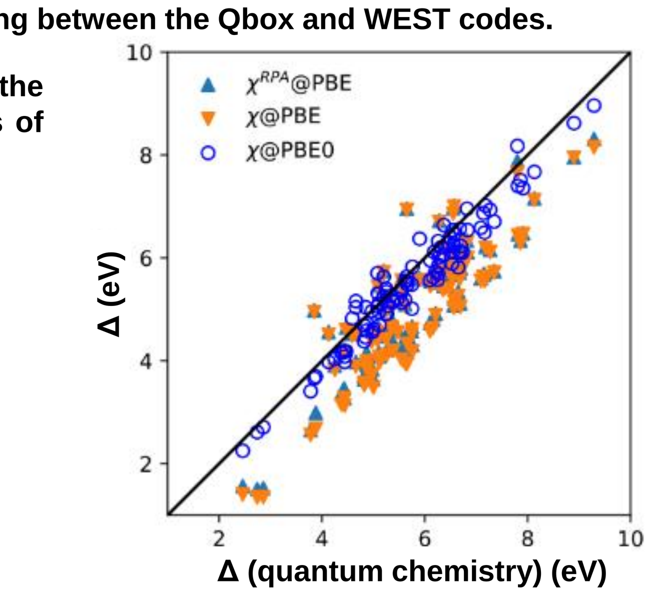


**By utilizing compact representations of Kohn-Sham wavefunctions (bisection orbitals) as implemented in the Qbox code, the computational cost of solving the BSE may be significantly reduced by neglecting pairs of orbitals with small overlap.**

**Orbital overlap:**

$$O_{ij} = \frac{\int |\varphi_i|^2 |\varphi_j|^2 dr}{\sqrt{\int |\varphi_i|^4 dr}\sqrt{\int |\varphi_j|^4 dr}}$$

**Optical absorption spectra of the $C_{60}$ molecule:**

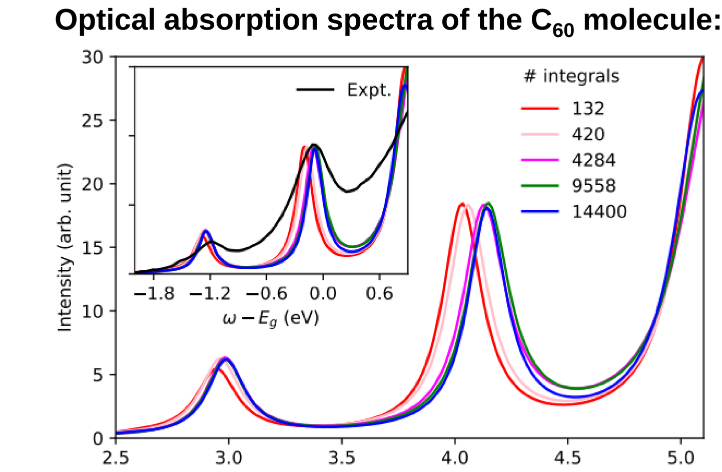


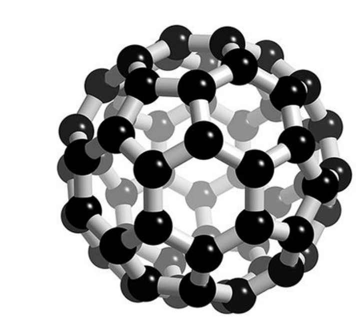

**By combining FPMD simulations with BSE and GW calculations, we computed the absorption spectra of ice and water close to ambient conditions. In particular, we computed the imaginary part of the macroscopic dielectric constant (Im[$\varepsilon_M$]) for water and ice by averaging over multiple snapshots of FPMD trajectories.**

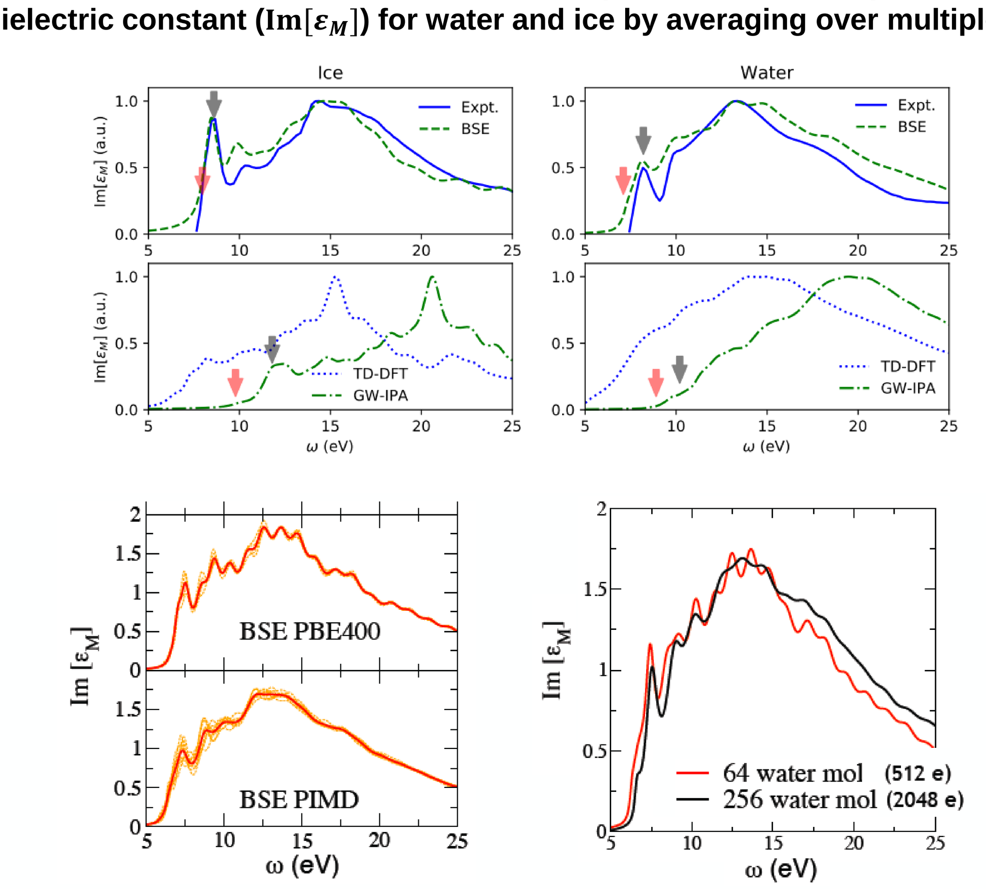


**Good agreement is found between GW-BSE and experiment both for the relative energy positions and intensities of the peaks over a wide range of energy.**

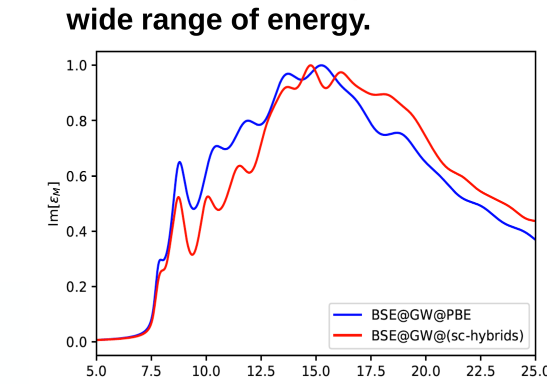


PBE400: www.quantum-simulation.org/reference/h2o/pbe400/s32/index.htm
PIMD: path integral MD. A. Gaiduk, T. A. Pham, M. Govoni, F. Paesani, G. Galli. *Nature Comm.* 2018
sc-hybrids: J. Skone, M. Govoni, G. Galli. *PRB.* 2014
Bisection algorithm: F. Gygi. *PRL.* 2009

## References and Acknowledgements

M. Govoni, G. Galli. *JCTC.* 2015. 11(6), 2680-2696.
P. Scherpelz, I. Hamada, M. Govoni, G. Galli. *JCTC.* 2017. 12(8), 3523-3544.
M. Govoni, G. Galli. *JCTC.* 2018. 14(4), 1895-1909.
H. Ma, M. Govoni, F.Gygi, G.Galli. 2018 (submitted).
L. N. Nguyen, H. Ma, M. Govoni, F.Gygi, G.Galli. 2018 (submitted).

Work supported by MICCoM, as part of the Computational Materials Sciences Program funded by the U.S. Department of Energy, Office of Science, Basic Energy Sciences, Materials Sciences and Engineering Division through Argonne National Laboratory, under contract number DE-AC02-06CH11357. We used computational resources from the National Energy Research Scientific Computing Center (NERSC), Argonne Leadership Computing Facility and University of Chicago Research Computing Center.